ACS APPLIED MATERIALS & INTERFACES

Research Article

www.acsami.org

Dynamic Modulation of Small-Sized Multicellular Clusters Using a Cell-Friendly Photoresist

Jong-Cheol Choi,[†] Hong-Ryul Jung,[‡] and Junsang Doh*[,†,‡]

[†]Department of Mechanical Engineering, [‡]School of Interdisciplinary Bioscience and Bioengineering (I-Bio), Pohang University of Science and Technology, San31, Hyoja-dong, Nam-Gu, Pohang, Gyeongbuk, 790-784, Korea

Supporting Information

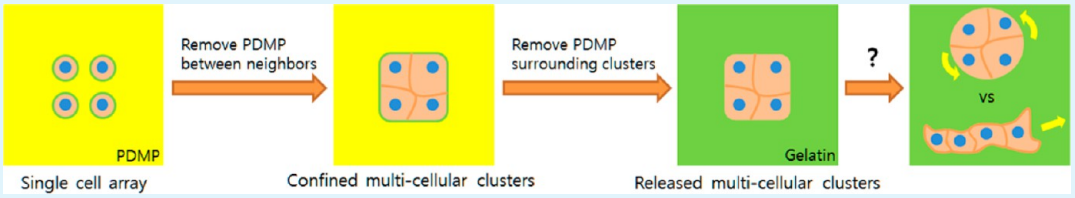

ABSTRACT: Dynamics of small-sized multicellular clusters is important for many biological processes including embryonic development and cancer metastasis. Previous methods to fabricate multicellular clusters depended on stochastic adhesion and proliferation of cells on defined areas of cell-adhering islands. This made precise control over the number of cells within multicellular clusters impossible. Variation in numbers may have minimal effects on the behavior of multicellular clusters composed of tens of cells but would have profound effects on groups with fewer than ten cells. Herein, we report a new dynamic cell micropatterning method using a cell-friendly photoresist film by multistep microscope projection photolithography. We first fabricated single cell arrays of partially spread cells. Then, by merging neighboring cells, we successfully fabricated multicellular clusters with precisely controlled number, composition, and geometry. Using this method, we generated multicellular clusters of Madin−Darby canine kidney cells with various numbers and initial geometries. Then, we systematically investigated the effect of multicellular cluster sizes and geometries on their motility behaviors. We found that the behavior of small-sized multicellular clusters was not sensitive to initial configurations but instead was determined by dynamic force balances among the cells. Initially, the multicellular clusters exhibited a rounded morphology and minimal translocation, probably due to contractility at the periphery of the clusters. For 2-cell and 4-cell clusters, single leaders emerged over time and entire groups aligned and comigrated as single supercells. Such coherent behavior did not occur in 8-cell clusters, indicating a critical group size led by a single leader may exist. The method developed in the study will be useful for the study of collective migration and multicellular dynamics.

KEYWORDS: *dynamic micropatterning, multicellular clusters, collective migration, cell-friendly photoresist*

INTRODUCTION

Recent development of surface chemistry and microfabrication has provided new opportunities to better understand behavior of multicellular clusters.[1,2] Surface micropatterning of cell-adhesion ligand (e.g., fibronectin, RGD peptide) islands surrounded by cell-repelling materials (e.g., poly(ethylene glycol), bovine serum albumin, etc.) can be used to create multicellular clusters with different sizes and shapes to examine various biophysical and biochemical factors critical for multicellular interactions.[3−6] However, the number of cells occupying identical sized islands within a surface may vary depending on local cell density and kinetics of cell adhesion/spreading. Variation in numbers may not be a serious issue for multicellular clusters composed of tens or hundreds of cells, but would be critical for small multicellular clusters composed of fewer than ten cells. Dynamic assembly and migration of multicellular clusters composed of fewer than ten cells have been observed in the processes of development and pathogenesis.[7,8] For example, during the oogenesis of *Drosophila melanogaster*, border cell clusters composed of six to ten cells coherently migrate toward an oocyte.[9] During cancer invasion and metastasis, moderately differentiated epithelial tumors form small-sized clusters and undergo collective migration.[10] Development of dynamic micropatterning techniques that allow fabrication of precisely controlled sizes and geometries would be useful to systematically study dynamics of small-sized multicellular clusters.

Various dynamic micropatterning methods based on electrochemistry,[11−15] photochemistry/photophysics,[3,16−19] and click-chemistry[20] have been developed to remove the cell-repelling materials or to convert cell-repelling materials to cell-adhesion ligands. Among them, methods based on light stimulation are the most suitable for in situ dynamic micropatterning because illumination of light can be readily achieved on selected areas of cell micropatterned surfaces during microscopy using light sources and optics of fluorescence microscopes. By ablating cell-repelling materials using high power pulsed lasers, shapes of cells were manipulated with submicrometer resolution in situ.[18]

Received: September 24, 2013
Accepted: November 20, 2013
Published: November 20, 2013

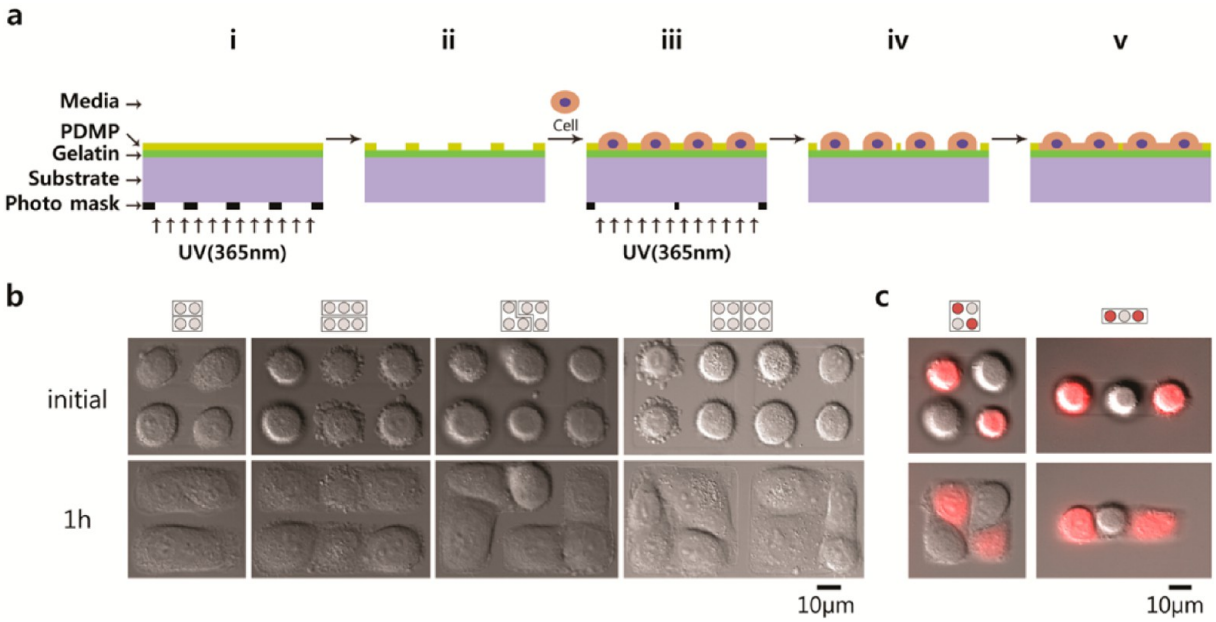

Figure 1. Fabrication of multicellular clusters from single cell arrays. (a) Schematic of multicellular cluster fabrication using single cell arrays. (b) Representative differential interference contrast (DIC) images of multicellular clusters of HeLa cells with various numbers and geometries. (c) Representative overlay images of DIC/red fluorescence of unlabeled and labeled HeLa cells.

Although this method allows for high-resolution dynamic micropatterning of cells, it cannot be applied to a large area because it is based on slow point scanning of focused laser beams. In contrast, microscope projection photolithography (MPP) based on arc lamps and gray photomasks printed on transparency films are better for large area high throughput dynamic patterning with micrometer scale resolution.[19,21]

In this study, we devised a new dynamic cell micropatterning technique by multistep MPP using a cell-friendly photoresist poly(2,2-dimethoxy nitrobenzyl methacrylate-*r*-methyl methacrylate-*r*-poly(ethylene glycol) methacrylate) (PDMP).[21] We first fabricated single cell arrays of partially spread cells. Then, by merging neighboring cells within the single cell arrays, multicellular clusters with precisely controlled size, composition, and geometry were successfully fabricated. Using this method, we systematically investigated the effects of sizes and initial geometries of small-sized multicellular clusters on their motility behaviors.

MATERIALS AND METHODS

PDMP Synthesis and Substrate Preparation. Random terpolymer PDMP (composition: 2,2-dimethoxy nitrobenzyl methacrylate ~42 wt %, methyl methacrylate ~24 wt %, and poly(ethylene glycol) methacrylate ~34 wt %, Mn ~ 6120 Da, PDI 1.34) was synthesized and characterized as described elsewhere.[21] Clean glass coverslips were coated with gelatin (Sigma) by incubating in a 0.1% geletin solution at room temperature for 30 min. Gelatin-coated coverslips were spincoated with 3 wt % of PDMP in 1,4-dioxane (Sigma) at 2000 rpm for 2 min to form ~100 nm thick film and baked at 100 °C for 24 h.

Fluorescence Microscope. A modified Olympus IX81 epifluorescence microscope with 40× (UPlanSApo, NA = 0.95) objective lens, and an iXon EM CCD camera was used for imaging and micropatterning. Lambda LS xenon lamp (175 W, Sutter Instrument) and DAPI (EX. 365, BS 395, EMBP 445/50) filter sets were used for illumination and fluorescence imaging. The microscope was automatically controlled, and the acquired images were analyzed and processed with Methamorph (Universal Imaging, Molecular Devices).

Microscope Projection Photolithography (MPP). Gelatin- and PDMP-coated and baked coverslips were loaded in a Chamlide magnetic chamber (Live Cell Instrument, Korea) filled with PBS. Then, the magnetic chambers were mounted on the microscope stage. Photomasks were printed on transparency films using a high-resolution image setter with 40 000 dpi resolution (Microtech Co., Ltd.) and inserted at the field diaphragm of the microscope. For UV illumination, the xenon lamp and DAPI filter described above were used. Microscope projection lithography was performed by exposing PDMP film with plane-focused UV though photomasks for 5 s.

Cell Culture. HeLa cells (a gift from Dr. Sung Ho Ryu, POSTECH) and MDCK cells (Korean cell line bank) were cultured in DMEM medium (Gibco) supplemented with 10% FBS (Gibco) and 1% penicillinestreptomycin (Invitrogen).

Multicellular Cluster Patterning. MPP was performed with a photomask containing arrays of circular spots (10 μm projected diameter) to dissolve PDMP in the UV-illuminated region and to expose the underlying gelatin layer. Then, 1 mL of HeLa or MDCK cells (5×10^5 cells/mL) suspended in growth media containing cell-cycle inhibitors (2 mM hydroxyurea and 1 μg/mL aphidicolin) were seeded onto the substrates and incubated in a tissue culture incubator for 2 h. A media containing cell-cycle inhibitors was used throughout the experiments to prevent cell division. By gently rinsing nonadhering cells, we obtained single cell arrays of cells. Then, we mounted single cell array-containing chambers on the microscope stage equipped with a Chamlide TC incubator system (maintaining 37 °C and 5% CO_2). A second photomask was inserted in the field diaphragm. The second photomask and single cell arrays cells were precisely registered by adjusting the position of the microscope stage, and 365 nm UV light was illuminated through the second photomask. Subsequently, bright field images were acquired every 1 min to monitor the spreading of single cells to form multicellular clusters.

RESULTS AND DISCUSSION

Fabrication of Multicellular Clusters with Precisely Controlled Sizes, Geometries, and Compositions. Multicellular clusters with precisely controlled shapes and cell numbers were fabricated as schematically shown in Figure 1a. Glass coverslips coated with gelatin, which promotes cell adhesion, were spincoated with a cell-friendly photoresist

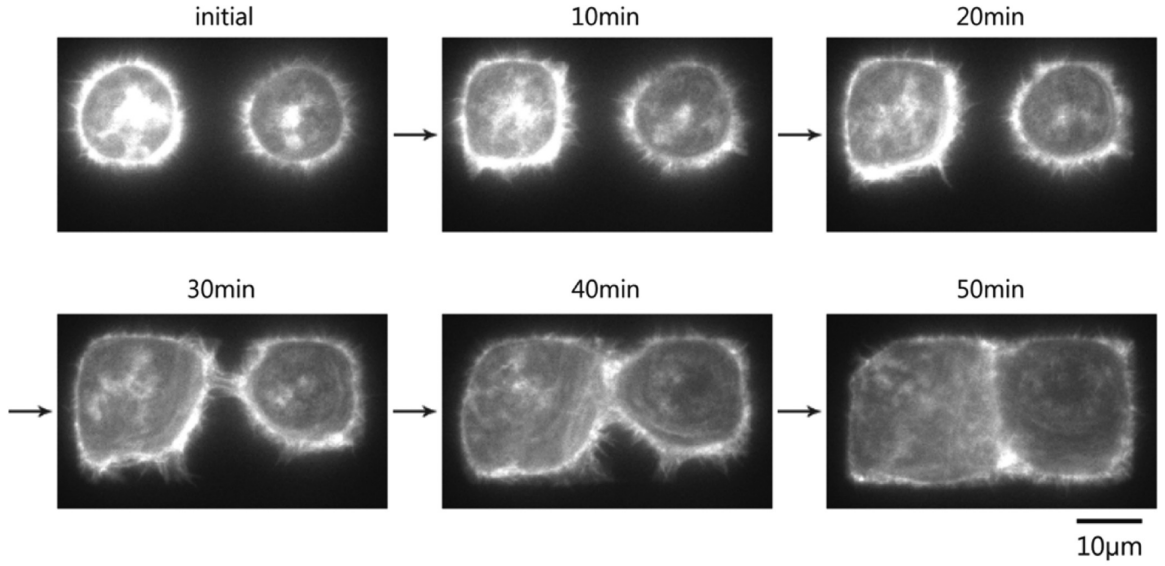

Figure 2. Time-lapse images of F-actin dynamics visualized by lifeact-GFP during adherens junction formation.

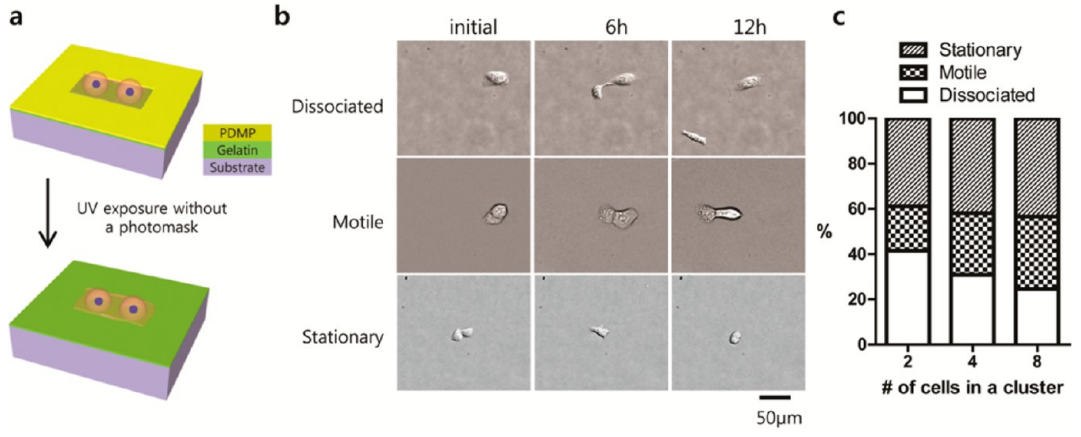

Figure 3. Characteristics of multicellular clusters released from confinement. (a) Experimental scheme. (b) Representative time-lapse images of 2-cell clusters of MDCK cells exhibiting different modes (dissociated, motile, and stationary). (c) Effect of multicellular size on the behavior of multicellular clusters.

PDMP[19,21] and loaded in a chamber filled with phosphate buffered saline (PBS). First, MPP was performed with a photomask containing arrays of circles with projected diameter 12 μm (Figure 1a(i)), which is slightly smaller than the diameter of HeLa cells (14.6 ± 1.6 μm) or Madin−Darby Canine Kidney (MDCK) cells (15.2 ± 1.7 μm) in suspension. Because PDMP thin films spontaneously dissolve in PBS upon illumination of UV at 365 nm, circular patches of gelatin layers surrounded by PDMP films were formed (Figure 1a(ii)). Then, cells suspended in culture media containing cell-cycle inhibitors (2 mM hydroxyurea and 1 μg/mL aphidicolin) were applied to the surface, incubated for 2 h, and rinsed to remove nonadhering cells (Figure 1a(iii)). Media containing cell-cycle inhibitors was used throughout the experiments to prevent cell division. Because PDMP does not allow cell adhesion and the gelatin island size is slightly smaller than the size of cells used, single cell arrays of cells were formed as previously demonstrated.[19] Subsequently, a single cell array-containing chamber was mounted to the microscope stage equipped with environmental chambers maintaining cell culture conditions (37 °C and 5% CO_2). A second photomask containing features that could cover various numbers of cells on single cell arrays, when projected through an objective lens, was inserted into the field diaphragm and registered with the cell array, and then the second MPP was performed (Figure 1a(iv)). Then, the initially adhered cells spontaneously spread to fill an area of freshly exposed gelatin layer resulting in multicellular cluster formation (Figure 1a(v)). Successfully fabricated multicellular clusters composed of two, three, and four cells in different geometries from single cell arrays are shown in Figure 1b. This method can be extended readily to fabricate multicellular clusters composed of multiple types of cells by repeating steps (ii) and (iii) multiple times and finally merging them. For example, to fabricate multicellular clusters composed of two different types of cells (unlabeled HeLa cells and red fluorophore-labeled HeLa cells) as shown in Figure 1c, single cell arrays of unlabeled and red fluorophore-labeled HeLa cells were created sequentially by repeating steps (ii) and (iii) twice, and neighboring unlabeled and red fluorophore-labeled HeLa cells were merged together by the third MPP. In this way, multicellular clusters with defined number, composition, and geometry were successfully fabricated. In addition, by using cells expressing GFP-fused molecules of interest, we were able to observe dynamics of molecules during adherens junction

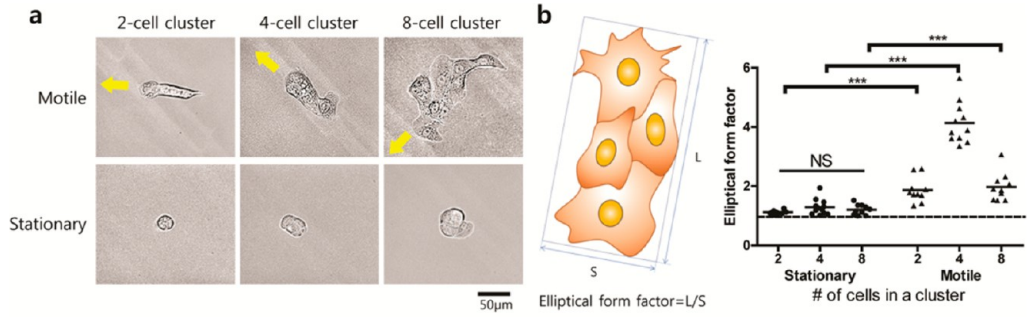

Figure 4. Morphology multicellular clusters in motile and stationary states. (a,b) Representative DIC images (a) and elliptical form factors (b) of motile and stationary of MDCK cells clusters of various numbers. Yellow arrows indicate migrating directions. White lines are drawn to mark boundaries of individual cells.

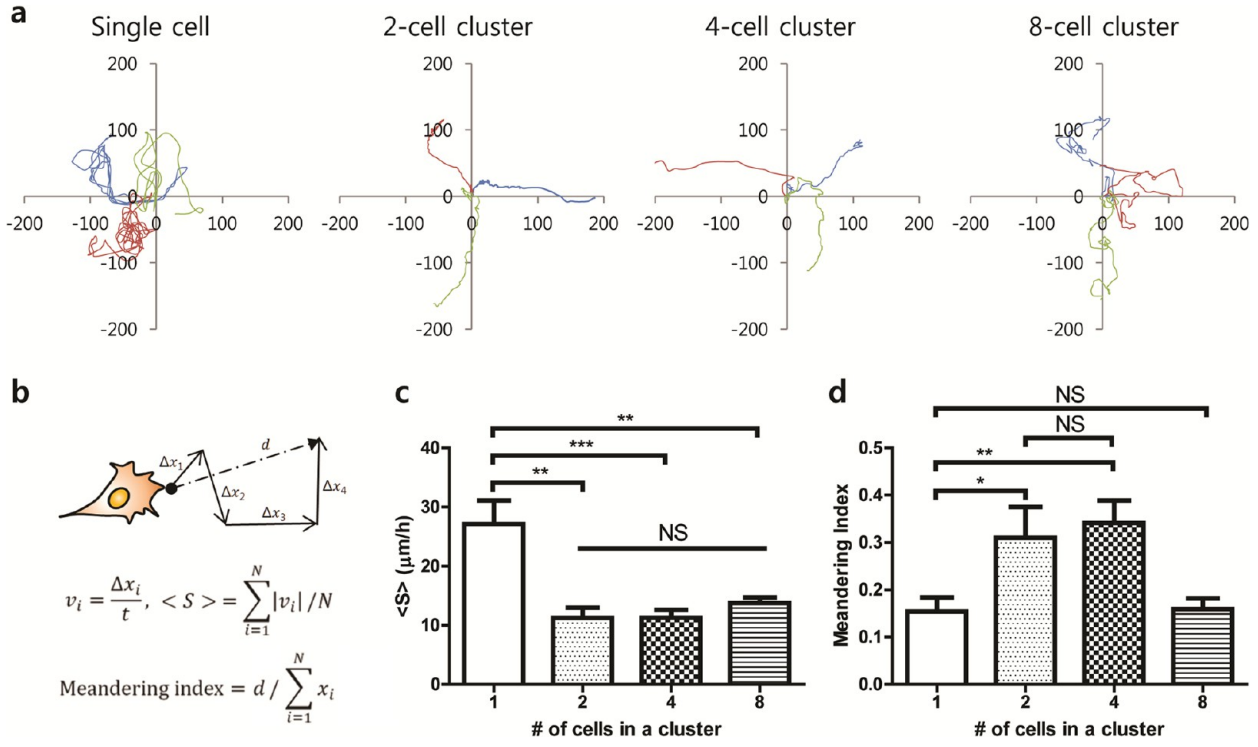

Figure 5. Dynamics of motile population of multicellular clusters. (a) Representative trajectories of single cells and multicellular clusters with various numbers of MDCK cells. Scale: μm. (b) Schematic definition of average speed and meandering index. (c,d) Average speed (c) and meandering index (d) of single and multicellular clusters of MDCK cells.

formation (Figure 2 and Movie S1 in the Supporting Information).

Characteristics of Multicellular Clusters Released from Confinement. Next, successfully formed multicellular clusters composed of a defined number of cells were confined in PDMP for 6 h to stabilize their adherens junction, and released by brief (~5 s) exposure to UV without a photomask to dissolve the PDMP films around them (Figure 3a). Three distinct behaviors emerged when the released multicellular clusters were observed by time-lapse microscopy over 36 h. First, individual cells in the multicellular clusters became dissociated and migrated separately, denoted by "dissociated" (top panel of Figure 3b and Movie S2 (Supporting Information)). Second, the multicellular clusters migrated together, denoted by "motile" (middle panel of Figure 3b and Movie S3 (Supporting Information)). Third, the multicellular clusters remained near their original locations with minimal net translocation, denoted by "stationary" (bottom panel of Figure 3b and Movie S4 (Supporting Information)). All the clusters of HeLa cells observed (twelve 2-cell clusters and eight 4-cell clusters) dissociated within 12 h when released from PDMP thin film confinement. In contrast, the majority of the clusters of MDCK cells stayed together over 36 h. To systematically assess the effect of size of the multicellular clusters on their behavior, 2-, 4-, and 8-cell MDCK clusters were created and released from PDMP confinement almost simultaneously by brief (~5 s) UV illumination without a photomask. Using a motorized stage, time-lapse images of 40–60 single cells/multicellular clusters were acquired every 20 min for 36 h in a single set of experiments. By pooling data from four independent experiments, a large number of data, sufficient for statistical analysis, was collected (n = 92 for single cells, n = 33 for 2-cell clusters, n = 43 for 4-cell clusters, and n = 31 for 8-cell clusters). Using these data, the behaviors of multicellular clusters were first assigned to one of the three categories described in Figure 3b and plotted in Figure 3c. As the number

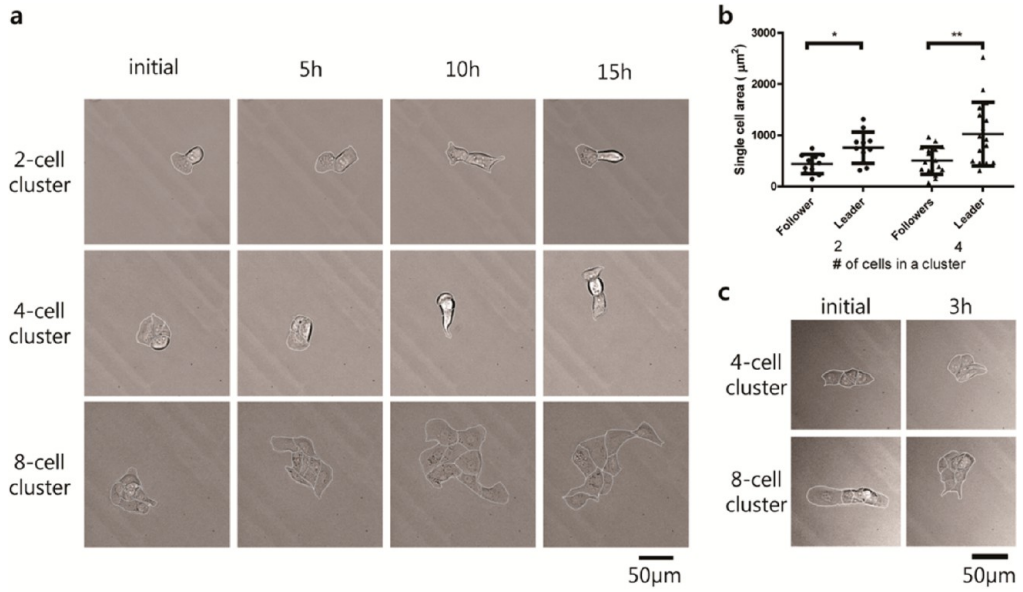

Figure 6. Characteristics of motile population of multicellular clusters. (a) Representative time-lapse images of motile MDCK clusters of various numbers. (b) Single cell area of leaders and followers in 2-cell and 4-cell clusters of MDCK cells. (c) Representative time-lapse images of 4-cell and 8-cell clusters with linear initial configuration. White lines are drawn to mark boundaries of individual cells.

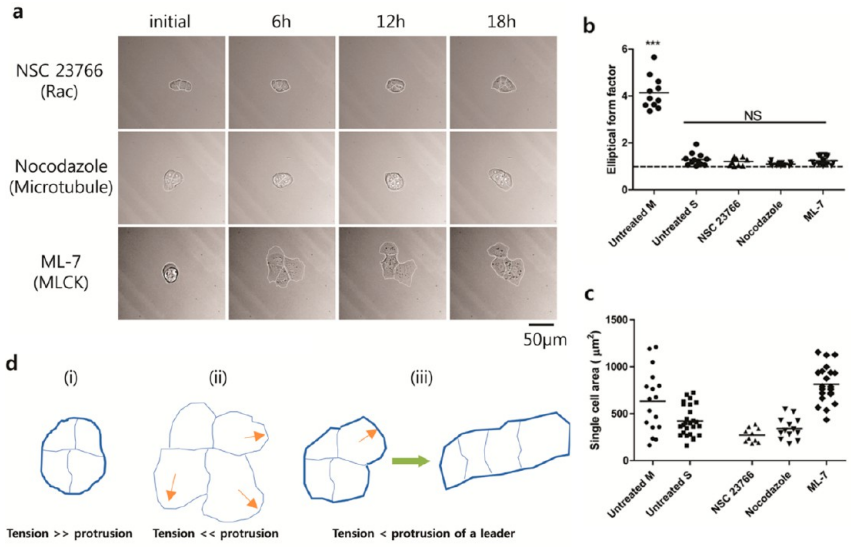

Figure 7. Effect of pharmacological inhibitors targeting actomyosin regulators on behavior of 4-cell clusters. (a) Representative time-lapse images of 4-cell clusters of MDCK cells treated with pharmacological inhibitors (targets). White lines are drawn to mark boundaries of individual cells. (b,c) Effect of inhibitors on elliptical form factor (b) and single cell area (c) of 4-cell clusters of MDCK cells. "M" means "motile" and "S" means "stationary". (d) Schematic model showing various behaviors of 4-cell clusters. The thickness of the lines surrounding cells represents the strength of contractility, and arrows indicate direction of protrusive forces. (i) 4-cells clusters with dominant peripheral contractility. Untreated stationary, Rac-inhibited, and microtubule-inhibit clusters correspond to this cartoon. (ii) 4-cell clusters lacking peripheral contractility. MLCK-inhibited clusters correspond to this cartoon. (iii) 4-cell clusters with a single leader. Motile clusters correspond to this cartoon.

of cells in the clusters increased, their stability also increased, possibly due to stronger multivalent interactions in clusters with larger numbers of cells.[22] Also, the percentage of motile clusters increased slightly as the sizes of the multicellular clusters increased. Of note, the shape of the multicellular clusters strongly depended on their motility status regardless of the number of cells. Motile multicellular clusters exhibited elongated shapes, whereas "stationary" multicellular clusters were mostly rounded (Figure 4a). These trends were assessed quantitatively by measuring the elliptical form factor (EFF), which is a widely used parameter to characterize elongation of single cells in response to various biophysical and biochemical cues,[23,24] as schematically shown in the left panel of Figure 4b. EFF values of stationary multicellular clusters were close to 1 for all the examined. In contrast, the EFF values of motile clusters depended on their sizes. Although all the EFF values of motile multicellular clusters were significantly greater than 1, average EFF values of motile 2- and 4-cell clusters were close to 2 and 4, respectively, meaning that the cells in those clusters formed approximately straight lines.

Size-Dependent Motility Behavior of Multicellular Clusters. The detailed dynamics of motile populations of

cells within clusters of different sizes was quantitatively analyzed by tracking the centroids of clusters over 36 h (Figure 5). Representative trajectories of the centroids of single cells and multicellular clusters of various sizes over 36 h were plotted in Figure 5a. Time-lapse images and movies of one example of each case are shown in Figure 6a and Movies S5−8 (Supporting Information), respectively. Although single cells and 8-cell clusters frequently changed directions, 2-cell and 4-cell clusters maintained their initial directions over long periods of time and exhibited persistent migration. Of note, cells in 2- and 4-cell clusters maintained epithelial characteristics, rounded morphologies with junctional integrity, and all the cells in the clusters aligned and exhibited coordinated motion in following one "leader" cell. In sharp contrast, cells in 8-cell clusters became thin and elongated, lost junctional integrity, and individual cells migrated without coordinating with neighboring cells, even while maintaining thin fibrous connections, which are characteristics of epithelial-mesenchymal transition.[25] In 2-cell and 4-cell clusters where single leaders emerged over time and led each group, the area of leader cells was significantly greater than that of the follower cells (Figure 6b). To test whether the initial geometry of multicellular clusters affected motility or leader formation, 4-cell and 8-cell clusters were initially linearly aligned and released. Interestingly, the majority of multicellular clusters (30/35 for 4-cell clusters and 9/10 for 8-cell clusters) shrank within 3 h to spherical shapes with EFF close to 1, potentially driven by the strong intracellular adhesion forces and contractility,[26] rather than underwent collective migration led by cells at the ends of initial linear geometry (Figure 6c and Movies S9 and S10 (Supporting Information)). This result indicates that multicellular clusters composed of fewer than ten cells can quickly reach dynamic force equilibrium, and the effect of initial conditions is minimal. In sharp contrast, as examined in the previous study, for the case of multicellular clusters composed of more than ten cells of MDCK cells, the initial geometry determined leader cell formation.[3]

Effects of Pharmacological Inhibitor Treatment on the Dynamics of Multicellular Clusters. To gain mechanistic insights into the phenomena described above, pharmacological inhibitors against key molecules regulating protrusive and contractile forces were added to 4-cell clusters of MDCK cells 1 h before removing PDMP films surrounding them, and their behaviors were monitored by time-lapse microscopy. When Rac, which mediates actin-polymerization driven membrane protrusion at leading edges,[27] was inhibited by NSC23766, all the observed multicellular clusters (n = 10) exhibited a rounded appearance with EFF close to 1 (Figure 7b), and rotated around the original positions with minimal net translocation (top panel of Figure 7a and Movie S11 (Supporting Information)). When they were treated with nocodazole, which indirectly enhances contractility by releasing microtubule-bound GEF-H1 to activate RhoA,[28] all the clusters examined (n = 13) behaved similarly to Rac-inhibited clusters (middle panel of Figure 7a and Movie S12 (Supporting Information)). These results indicate that balancing between contraction and protrusion determines a motile or stationary state. As reported previously, multicellular clusters exert traction forces at their boundaries, not near intercellular junctions.[29,30] Therefore, when contractile forces dominate or protrusive forces are weak, multicellular clusters would be expected to have rounded shapes with EFF close to 1, with minimal translocation as schematically drawn in Figure 7d(i). Leader cells may emerge by overcoming peripheral contractility via Rac-mediated protrusion.[31,32] To test whether releasing peripheral contractility is sufficient for leader formation and collective migration, we inhibited myosin light chain kinase (MLCK) with ML-7. Cells in clusters treated with ML-7 showed only sporadic protrusion, exhibited more spread morphologies than untreated stationary clusters (Figure 7c) due to loss of peripheral contractility, but none of them lined up and collectively migrated following single leaders (bottom panel of Figure 7a and Movie S13 (Supporting Information)). Instead, all the clusters examined (n = 24) exhibited EFF close to 1 and minimal translocation. This result suggests that protrusion by one cell in the absence of peripheral contraction cannot be propagated throughout entire multicellular clusters to result in collective migration, as schematically drawn in Figure 7d(ii). Taken together, none of multicellular cluster treated with inhibitors exhibited collective migration lead by a leader, suggesting leader cell formation and corporative migration require fine balancing between protrusion and contraction both local and global levels as schematically shown in Figure 7d(iii).[8,33,34]

CONCLUSION

Multicellular clusters composed of various numbers of cells in different geometries were fabricated previously, but the number of cells in these clusters was stochastically determined, rather than precisely controlled. To overcome this limitation, we started with single cell arrays, and by merging neighboring cells within single cell arrays, we could fabricate multicellular clusters composed of fewer than ten cells with precisely defined number, geometry, and composition. Compared with multicellular clusters composed of more than ten cells, the effect of initial geometry was minimal, and the behavior of multicellular clusters was more dynamically determined by force balancing among cells. In addition, coherent migration led by a single leader was observed for 2-cell and 4-cell clusters, but such coordination did not occur in 8-cell clusters. The method developed in this study will be useful for the study of collective migration and multicellular dynamics.

ASSOCIATED CONTENT

Supporting Information

Time-lapse movie of F-actin dynamics during adherens junction formation. Representative movies of small-sized multicellular clusters. This material is available free of charge via the Internet at http://pubs.acs.org.

AUTHOR INFORMATION

Corresponding Author

*Junsang Doh. Address: San31, Hyoja-dong, Nam-Gu, Pohang, Gyeongbuk, 790-784, Korea. Tel: +82-54-279-2189. Fax: +82-54-279-3199. E-mail: jsdoh@postech.ac.kr.

Author Contributions

J.C.C. performed experiments, analyzed data, and participated in experimental design and manuscript writing. H.R.J. assisted cell experiments and did lifeact-GFP transfection. J.D. established initial questions and wrote manuscript and participated in experimental design.

Notes

The authors declare no competing financial interest.

■ ACKNOWLEDGMENTS

This work was supported by a grant of the Korea Healthcare Technology R & D Project, Ministry for Health, Welfare and Family Affairs, Republic of Korea (J.D., Grant No. A121177/HI12C1079).

■ REFERENCES

(1) Chen, C. S.; Jiang, X.; Whitesides, G. M. *MRS Bull.* **2005**, *30* (3), 194−201.
(2) Théry, M. *J. Cell Sci.* **2010**, *123* (24), 4201−4213.
(3) Rolli, C. G.; Nakayama, H.; Yamaguchi, K.; Spatz, J. P.; Kemkemer, R.; Nakanishi, J. *Biomaterials* **2012**, *33* (8), 2409−2418.
(4) Kumar, G.; Chen, B.; Co, C. C.; Ho, C. C. *Exp. Cell Res.* **2011**, *317* (10), 1340−52.
(5) Doh, J.; Kim, M.; Krummel, M. F. *Biomaterials* **2010**, *31* (12), 3422−3428.
(6) Nelson, C. M.; Jean, R. P.; Tan, J. L.; Liu, W. F.; Sniadecki, N. J.; Spector, A. A.; Chen, C. S. *Proc. Natl. Acad. Sci. U. S. A.* **2005**, *102* (33), 11594−11599.
(7) Friedl, P.; Gilmour, D. *Nat. Rev. Mol. Cell Biol.* **2009**, *10* (7), 445−57.
(8) Montell, D. J. *Science* **2008**, *322* (5907), 1502−1505.
(9) Montell, D. J.; Yoon, W. H.; Starz-Gaiano, M. *Nat. Rev. Mol. Cell Biol.* **2012**, *13* (10), 631−645.
(10) Friedl, P.; Alexander, S. *Cell* **2011**, *147* (5), 992−1009.
(11) Li, Y.; Yuan, B.; Ji, H.; Han, D.; Chen, S.; Tian, F.; Jiang, X. *Angew. Chem., Int. Ed.* **2007**, *46* (7), 1094−1096.
(12) Zhao, C.; Witte, I.; Wittstock, G. *Angew. Chem., Int. Ed.* **2006**, *45* (33), 5469−5471.
(13) Inaba, R.; Khademhosseini, A.; Suzuki, H.; Fukuda, J. *Biomaterials* **2009**, *30* (21), 3573−3579.
(14) Jiang, X.; Ferrigno, R.; Mrksich, M.; Whitesides, G. M. *J. Am. Chem. Soc.* **2003**, *125* (9), 2366−2367.
(15) Yousaf, M. N.; Houseman, B. T.; Mrksich, M. *Angew. Chem., Int. Ed.* **2001**, *40* (6), 1093−1096.
(16) Auernheimer, J.; Dahmen, C.; Hersel, U.; Bausch, A.; Kessler, H. *J. Am. Chem. Soc.* **2005**, *127* (46), 16107−16110.
(17) Nakanishi, J.; Kikuchi, Y.; Inoue, S.; Yamaguchi, K.; Takarada, T.; Maeda, M. *J. Am. Chem. Soc.* **2007**, *129* (21), 6694−6695.
(18) Vignaud, T.; Galland, R.; Tseng, Q.; Blanchoin, L.; Colombelli, J.; Théry, M. *J. Cell Sci.* **2012**, *125* (9), 2134−2140.
(19) Choi, J. C.; Doh, J. *Lab Chip* **2012**, *12* (23), 4964−4967.
(20) Van Dongen, S. F. M.; Maiuri, P.; Marie, E.; Tribet, C.; Piel, M. *Adv. Mater.* **2013**, *25* (12), 1687−1691.
(21) Kim, M.; Choi, J. C.; Jung, H. R.; Katz, J. S.; Kim, M. G.; Doh, J. *Langmuir* **2010**, *26* (14), 12112−12118.
(22) Mammen, M.; Choi, S. K.; Whitesides, G. M. *Angew. Chem., Int. Ed.* **1998**, *37* (20), 2754−2794.
(23) Karuri, N. W.; Liliensiek, S.; Teixeira, A. I.; Abrams, G.; Campbell, S.; Nealey, P. F.; Murphy, C. J. *J. Cell Sci.* **2004**, *117* (15), 3153−3164.
(24) Cukierman, E.; Pankov, R.; Stevens, D. R.; Yamada, K. M. *Science* **2001**, *294* (5547), 1708−1712.
(25) de Rooij, J.; Kerstens, A.; Danuser, G.; Schwartz, M. A.; Waterman-Storer, C. M. *J. Cell Biol.* **2005**, *171* (1), 153−64.
(26) Manning, M. L.; Foty, R. A.; Steinberg, M. S.; Schoetz, E. M. *Proc. Natl. Acad. Sci. U. S. A.* **2010**, *107* (28), 12517−12522.
(27) Ridley, A. J.; Schwartz, M. A.; Burridge, K.; Firtel, R. A.; Ginsberg, M. H.; Borisy, G.; Parsons, J. T.; Horwitz, A. R. *Science* **2003**, *302* (5651), 1704−1709.
(28) Chang, Y. C.; Nalbant, P.; Birkenfeld, J.; Chang, Z. F.; Bokoch, G. M. *Mol. Biol. Cell* **2008**, *19* (5), 2147−53.
(29) Mertz, A. F.; Banerjee, S.; Che, Y.; German, G. K.; Xu, Y.; Hyland, C.; Marchetti, M. C.; Horsley, V.; Dufresne, E. R. *Phys. Rev. Lett.* **2012**, *108* (19), 198101.
(30) Maruthamuthu, V.; Sabass, B.; Schwarz, U. S.; Gardel, M. L. *Proc. Natl. Acad. Sci. U. S. A.* **2011**, *108* (12), 4708−4713.
(31) Wang, X.; He, L.; Wu, Y. I.; Hahn, K. M.; Montell, D. J. *Nat. Cell Biol.* **2010**, *12* (6), 591−597.
(32) Inaki, M.; Vishnu, S.; Cliffe, A.; Rørth, P. *Proc. Natl. Acad. Sci. U. S. A.* **2012**, *109* (6), 2027−2032.
(33) Hidalgo-Carcedo, C.; Hooper, S.; Chaudhry, S. I.; Williamson, P.; Harrington, K.; Leitinger, B.; Sahai, E. *Nat. Cell Biol.* **2011**, *13* (1), 49−58.
(34) Khalil, A. A.; Friedl, P. *Integr. Biol.* **2010**, *2* (11−12), 568−574.